LANGMUIR Article
Cite This: Langmuir 2018, 34, 5163−5168
pubs.acs.org/Langmuir

Effect of Wetting on Drop Splashing of Newtonian Fluids and Blood

T. C. de Goede,*[,†] N. Laan,[†] K. G. de Bruin,[†,‡] and D. Bonn*[,†]

[†]Van der Waals-Zeeman Institute, Institute of Physics, University of Amsterdam, Science Park 904, 1098 XH Amsterdam, Netherlands

[‡]Netherlands Forensic Institute, Laan van Ypenburg 6, 2497 GB The Hague, Netherlands

ABSTRACT: We investigate the impact velocity beyond which the ejection of smaller droplets from the main droplet (splashing) occurs for droplets of different liquids impacting different smooth surfaces. We examine its dependence on the surface wetting properties and droplet surface tension. We show that the splashing velocity is independent of the wetting properties of the surface but increases roughly linearly with increasing surface tension of the liquid. A preexisting splashing model and simplification are considered that predict the splashing velocity by incorporating the air viscosity. Both the splashing model and simplification give a good prediction of the splashing velocity for each surface and liquid, demonstrating the robustness of the splashing model. We also show that the splashing model can also predict the splashing velocity of blood, a shear-thinning fluid.

INTRODUCTION

When impacting a dry, smooth surface, a droplet either spreads over the surface (for low-impact velocities) or disintegrates into smaller droplets (for high-impact velocities). This so-called splashing phenomenon has been the subject of numerous studies over the last several decades and is of relevance for a wide range of practical applications such as crop spraying,[1,2] rain drops impacting porous stones,[3,4] and forensic research.[5−7] The splashing velocity v_{sp} is defined as the critical value of the impact velocity of the droplet beyond which splashing occurs (Figure 1). Many studies have tried to find an

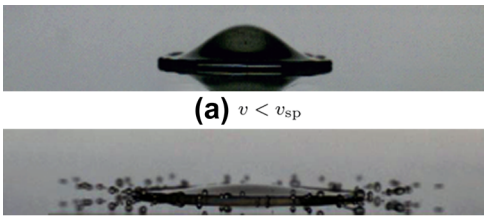

Figure 1. (a) Droplet impact for $v < v_{sp}$ where no splashing occurs. (b) Droplet impact for $v \geq v_{sp}$ where splashing occurs.

empirical relation between the splashing velocity and fluid parameters[8−13] and between the splashing velocity and surface properties.[14−17] In addition, Xu et al.[18] showed that the atmospheric conditions have a significant influence on droplet splashing,[13,17,19] implying that the air viscosity is also an important parameter. To include the air viscosity, Riboux and Gordillo recently proposed a theoretical model for impact and splashing on smooth surfaces.[20] They postulated that splashing occurs because of the breakup of a small liquid film that lifts off the surface just after the impact due to the lift force generated by the surrounding air. In the model, the fluid and substrate properties govern the splashing as well as the air viscosity; in ref 20, a quantitative agreement was found between the model and experiments on a single substrate.

Numerous experimental studies have investigated splashing;[8−19] however, the influence of the wetting properties of the surface on splashing has not been considered in detail. It has recently been shown that the wetting properties of the surface affect droplet spreading at low-impact velocities.[21,22] In the model of Riboux and Gordillo, the splashing velocity also depends on the surface properties.[20] The surface tension and the wetting properties of the surface are closely linked through Young's law.[23] Therefore, the dependence of the splashing velocity on surface tension should also be taken into account for a droplet of a given size. Furthermore, the splashing model has not yet been tested for more complex fluids such as, for example, blood. In forensics, being able to determine when blood splashes could help in distinguishing between the stains that are formed from the droplet impact (impact stain) or the stains formed by absorbing blood during contact with a blood source (transfer stain).[7,24] Blood is a shear-thinning fluid, but studies have shown that blood can be approximated as a Newtonian fluid when it is subjected to high shear rates.[25−27] Laan et al. showed in 2014 that the spreading of blood is similar to the spreading of Newtonian fluids, which was attributed to the high shear rate inside the droplet during spreading.[21] As splashing occurs during spreading (Figure 1b), the questions are whether blood can also be approximated as a Newtonian fluid during splashing and whether the splashing velocity of blood can also be predicted using the splashing model for Newtonian fluids of ref 20.

In this paper, we systematically investigate the effect of surface tension of the liquid and the wetting properties of the surface on the splashing velocity of the droplet. Using high-

Received: October 31, 2017
Revised: December 11, 2017
Published: December 13, 2017

DOI: 10.1021/acs.langmuir.7b03355
Langmuir 2018, 34, 5163−5168

speed camera footage, we measure the splashing velocity of a set of Newtonian ethanol–water mixtures and shear-thinning blood impacting on different surfaces at laboratory conditions. We compare the results with the splashing model of Riboux and Gordillo.[20] We show that the splashing model predicts the splashing of both ethanol–water mixtures and blood very well. Although the model is consistent with the experimental data, the calculation is complex and depends on several parameters that have to be inferred from the experimental conditions and have to be calculated separately. We therefore use a simplification, also given by Riboux and Gordillo, valid for low Ohnesorge numbers and atmospheric conditions, which is the situation that pertains to most practical applications and show that it predicts the splashing velocity very well. These results show that the splashing velocity is independent of the surface wetting properties and that blood can be approximated as a Newtonian fluid during splashing.

MATERIALS AND METHODS

To measure the splashing velocity v_{sp}, droplet impacts were recorded using a high-speed camera (Phantom Miro M310). The droplets were generated from a blunt-tipped needle (needle diameter 0.4 mm) using a syringe pump, where the needle was suspended above the substrate at a certain height. By systematically increasing the height of the needle and checking whether the droplet merely spreads over the surface (Figure 1a) or splashes (Figure 1b) for each height, we determined the initial droplet diameter D_0 and impact velocity v at the onset of splashing for each liquid. The fluid parameters of each liquid are given in Table 1. Three different surfaces were investigated for the ethanol–water mixtures: stainless steel, glass (Objektträger, Menzel Glaser, Thermo Scientific), and parafilm. All three surfaces were considered smooth, each having an arithmetic average roughness R_a below 0.5 μm.[22] For blood, the splashing velocity was determined from blood droplet impact footage on glass ($\theta_{st} \approx 20°$; where θ_{st} is the static contact angle of water[21]), acrylic glass [poly(methyl methacrylate), PMMA; $\theta_{st} \approx 70°$], Trespa ($\theta_{st} \approx 82°$), and polyoxymethylene (POM; $\theta_{st} \approx 79°$) surfaces using the data of ref 21. The density (1055 kg/m^3), surface tension (59 mN/m), and viscosity (4.8 mPa·s) of the blood used are also given by Laan et al.[21] Both the impacts of Newtonian fluids and blood were measured at 21 °C and atmospheric pressure. During the experiments with blood, the anti-coagulant ethylenediaminetetraacetic acid was added to prevent the coagulation of blood.

Table 1. Ethanol Mass Fraction, Density, Surface Tension, and Viscosity Values of Water, Ethanol, and Ethanol–Water Mixtures Used in This Study[a]

wt (%)	density (kg/m^3)	surface tension (mN/m)	viscosity (mPa·s)
0	997.0	72.0	0.89
5	989.0	56.4	1.23
10	981.9	48.1	1.50
15	975.3	42.7	1.82
20	968.7	38.0	2.14
40	935.3	30.2	2.85
60	891.1	26.2	2.55
80	843.6	23.8	1.88
100	789.3	21.8	1.20

[a]Source: refs 28 and 29.

RESULTS AND DISCUSSION

For each ethanol–water mixture, the contact angle θ on steel, glass, and parafilm was measured using the sessile drop method.[30,31] Because of surface inhomogeneities, a droplet deposited on a surface does not have a unique contact angle but attains a contact angle that ranges between the advancing (θ_a) and receding (θ_r) contact angle.[32] In Figure 2a, θ_a is plotted as a function of the surface tension. In glass, the contact angles of each fluid were too small to be determined. Therefore, each fluid is considered to be completely wetting the glass surface ($\theta_a \approx 0°$). Do note that the glass used in this study has a lower contact angle compared to the glass used in the study of ref 21. All liquids have a similar receding angle of roughly 20° when deposited on steel. When deposited on parafilm, the receding contact angles of all liquids were consistently 10° lower than their corresponding advancing angle.

To characterize the difference in wetting properties of the three substrates, Young's law is used, which describes the force balance between the interfacial tensions of the substrate, liquid droplet, and the surrounding vapor[23,33]

$$\sigma_{SV} - \sigma_{SL} = \sigma_{LV} \cos(\theta) \quad (1)$$

where σ_{LV} is the liquid–vapor interfacial tension of the liquid. σ_{SV} and σ_{SL} are the solid–vapor and solid–liquid interfacial tensions, respectively. Zisman assumed that the difference between σ_{SV} and σ_{SL} is a property of the solid that gives the surface free energy of the substrate.[23,31,34] $(\sigma_{SV} - \sigma_{SL})$ can be determined by finding the critical surface tension from the contact angle measurements: the surface tension at which a

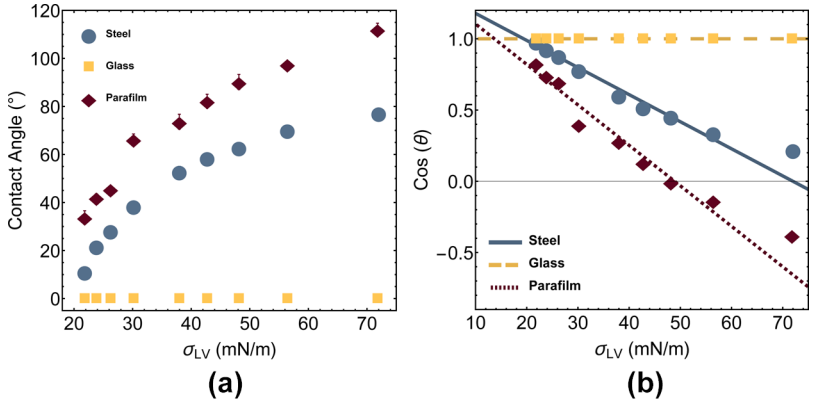

Figure 2. (a) Advancing contact angle as a function of surface tension for steel (blue circles), glass (yellow squares), and parafilm (red diamonds) substrates. (b) Cosine of θ_a as a function of surface tension. The blue solid, yellow dashed, and red dotted lines depict the linear fits of the static contact angles for water, glass, and parafilm, respectively.

DOI: 10.1021/acs.langmuir.7b03355
Langmuir 2018, 34, 5163–5168

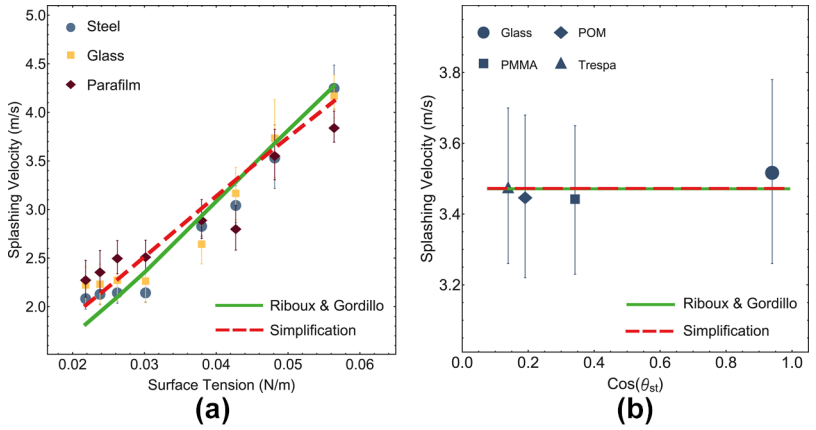

Figure 3. (a) Measured splashing velocity as a function of surface tension for stainless steel (blue circles) and borosilicate glass (yellow squares). The green line depicts the splashing velocity as given by the full splashing model [eq 6], whereas the red dashed line shows the splashing velocity as calculated from the simplified model [eq 14]. (b) Measured splashing velocity of blood (dark blue) for glass (circle), PMMA (square), POM (diamond), and Trespa (triangle) compared to the predicted splashing velocity of the full splashing model (open green symbols) and simplification (open red symbols).

droplet completely wets the surface. By plotting the cosine of the measured contact angles as a function of surface tension (Figure 2b), $(\sigma_{SV} - \sigma_{SL})$ is found by fitting a straight line through the data using the least squares method and extrapolating the fits to the surface tension for which the liquid would fully wet the surface ($\cos(\theta) = 1$). Because glass is completely wetted by all evaluated liquids, the critical surface tension of glass is higher than 71.99 mN/m. For steel and parafilm, a critical surface tension of 14 ± 1 and 19 ± 1 mN/m is found, respectively. Therefore, liquids wet the parafilm less compared to the steel surface.

The measured splashing velocities of the ethanol−water mixtures are plotted as a function of liquid surface tension in Figure 3a. The graph shows that the splashing velocity increases roughly linearly with the surface tension. For pure water droplets, no splashing was observed within the velocity range investigated here ($0.1 < v < 4.7$ m/s). No significant difference between the three evaluated surfaces is observed, implying that the splashing velocity is independent of the wetting properties of the substrate. The same holds for blood (Figure 3b), where the splashing velocity remains constant (~3.47 m/s) for all observed substrates. These results suggest that the wetting properties of the substrate do not influence the splashing velocity of both ethanol−water mixtures and blood, which is the first useful conclusion. This is remarkable as the droplet is in full contact with the substrate during splashing.[35,36] However, in ref 35, it was also observed that just before splashing, the edge of the liquid sheet dewets the surface from which the satellite droplets are formed (see Figure 4a−d).

Although surface roughness is not considered in this paper, it can also influence splashing.[16,17] On rough surfaces, the liquid sheet does not detach from the surface prior to breakup, giving rise to a different splash known as a "prompt splash".[9,17] The influence of surface roughness was not considered in the splashing model of ref 20. How the surface roughness can be incorporated into the splashing model is currently unknown and beyond the scope of this paper.

To describe splashing, in ref 20, the ejection time t_e (the moment a thin liquid sheet appears from the droplet after impact) is first calculated numerically using the momentum balance equation

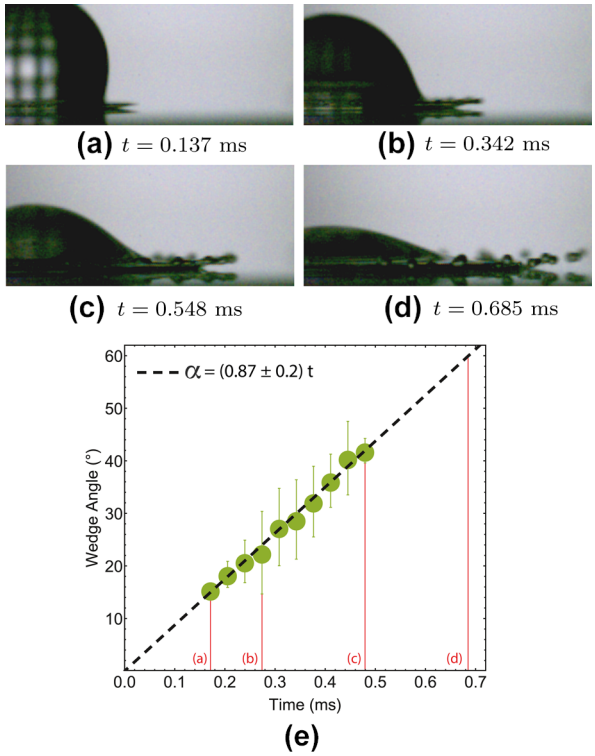

Figure 4. (a−d) High-speed camera footage of the lifted liquid sheet after impact (with $t = 0$ s, the moment of droplet impact). (e) Averaged measured wedge angle α (green circles) as a function of time on stainless steel. The error bar is given by the SD. The black dotted line is the best linear fit of wedge angle measurements. The vertical red lines depict the different stages of liquid sheet spreading as given in (a−d): the emergence of the liquid sheet from the droplet (a), radial expansion (b), formation of liquid fingers at the front of the liquid (c), and droplet detachment (d).

$$\frac{\sqrt{3}}{2} Re^{-1} t_e^{-1/2} + Re^{-2} Oh^{-2} = 1.21 t_e^{3/2} \quad (2)$$

where $\mathrm{Re} = \frac{\rho R v}{\mu}$ and $\mathrm{Oh} = \frac{\mu}{\sqrt{\rho R \sigma}}$ are the Reynolds and Ohnesorge numbers, respectively; ρ is the density, μ is the viscosity, σ is the surface tension of the liquid (equal to σ_{LV}), R

DOI: 10.1021/acs.langmuir.7b03355
Langmuir 2018, 34, 5163−5168

is the radius ($D_0/2$), and v is the impact velocity of the droplet. Using the ejection time, the velocity V_t and thickness H_t of the thin liquid sheet can be calculated

$$V_t = \frac{1}{2}\sqrt{3}\, v t_e^{-1/2} \tag{3a}$$

$$H_t = \frac{\sqrt{12}}{\pi} R t_e^{3/2} \tag{3b}$$

Using the sheet velocity and thickness, the aerodynamic lifting force, consisting of the suction ($\sim K_l \mu_g V_t$) and lubrication forces ($\sim K_u \rho_g V_t^2 H_t$), can then be determined. Here, μ_g and ρ_g are the viscosity and density of the air, respectively. The suction force is caused by the negative pressure difference above the liquid sheet due to the Bernoulli principle, whereas the lubrication force is generated by the air moving underneath the liquid sheet, creating a positive pressure difference that pushes the lamella upward. K_u and K_l are constants. While $K_u \approx 0.3$ was determined in ref 20 by numerical calculations, K_l can be calculated using the sheet thickness, mean free path of the molecules λ in the surrounding air, and wedge angle α, which is the angle between the lifted sheet and the surface

$$K_l = -\frac{6}{\tan^2 \alpha}\left(\ln\left(19.2\frac{\lambda}{H_t}\right) - \ln\left(1 + 19.2\frac{\lambda}{H_t}\right)\right) \tag{4}$$

According to ref 20, the wedge angle is equal to 60° and should be dependent on the wetting properties of the surface.[20]

Having determined these parameters, a dimensionless number defined as the splashing ratio β is calculated, which indicates the magnitude of the aerodynamic forces needed to overcome the surface tension to break up the liquid sheet into smaller droplets

$$\beta = \left(\frac{K_l \mu_g V_t + K_u \rho_g V_t^2 H_t}{2\sigma}\right)^{1/2} \tag{5}$$

Comparing eqs 2 and 5 to both their own experiments and previous work,[13,18,37] Riboux and Gordillo determined that the value of the splashing ratio should be around 0.14.

To calculate the splashing velocity from the splashing model of Riboux and Gordillo, eq 2 is rewritten as a quadratic equation for the splashing velocity v_{sp}, as a function of the fluid parameters and the ejection time

$$v_{sp} = \frac{\frac{\sqrt{3}}{2}\frac{\mu}{\rho R} t_e^{-1/2} + \sqrt{\frac{3}{4}\left(\frac{\mu}{\rho R}\right)^2 t_e^{-1} + 4.84\frac{\sigma}{\rho R} t_e^{3/2}}}{2.42 t_e^{3/2}} \tag{6}$$

To compare the splashing model with our experiments, eqs 3a and 3b are substituted into eq 5

$$\frac{3\sqrt{3}}{2\pi} R t_e^{1/2} v_{sp}^2 + \frac{\sqrt{3}}{2} K_l \mu_g t_e^{-1/2} v_{sp} - 2\sigma\beta^2 = 0 \tag{7}$$

Using eqs 6 and 7, the ejection time can be determined numerically, which in turn can be used to calculate the splashing velocity. For both Newtonian fluids and blood, the measured droplet radius was averaged. The best fit of the splashing model on our data (green line, Figure 3a,b) was determined by minimizing the sum of square residuals using the splashing ratio as a fit parameter. The obtained best fit value is equal to 0.135 ± 0.008, which is close to the value 0.14 found by Riboux and Gordillo. The error on the splashing ratio is determined by calculating the splashing ratio for each fluid and taking the SD of all splashing ratios. Previously, the splashing model was only verified for borosilicate glass substrates.[13,37] Here, we show that the splashing model can be universally applied to any smooth surface. Furthermore, the splashing model also accurately predicts the splashing velocities of blood (Figure 3b), where the splashing ratio of blood is nearly identical to the splashing ratio of the ethanol–water mixtures (β_{blood} = 0.141 ± 0.001). The fact that blood can be described with the splashing model of Riboux and Gordillo suggests that blood behaves as a Newtonian fluid during splashing, similar to droplet spreading.[21]

The wetting properties of the surface should, according to Riboux and Gordillo,[20] determine the wedge angle α. However, Riboux and Gordillo gave no explanation on why the value of the wedge angle should be 60°. To investigate the time dynamics of the wedge angle during splashing, we measure the wedge angle; in our experiments, we let ethanol droplets impact a stainless-steel surface at an impact velocity comparable to the splashing velocity ($v = v_{sp}$). Recording the impact with the high-speed camera gives the time evolution of liquid sheet expansion, which is depicted in Figure 4a–d. We observe that after the moment of the sheet ejection (Figure 4a), the liquid sheet starts to radially expand outward (Figure 4b). After a certain time, liquid fingers start to form at the edge of the sheet (Figure 4c), after which satellite droplets detach from the sheet (Figure 4d) and splashing occurs.

From each recorded frame, we extracted the instantaneous wedge angle, which is shown in Figure 4e. In this graph, the wedge angle seems to increase linearly with time until the moment of finger formation (Figure 4c). Assuming that the wedge angle keeps increasing linearly until droplet detachment, we can fit a simple linear function ($\alpha = At$) to the data of Figure 4e and extrapolate the wedge angle to the moment the droplets detach from the liquid sheet. Using this method, we obtain an average wedge angle of α = 59° ± 8° at the moment of droplet detachment (Figure 4d), which is similar to the value of the wedge angle postulated by Riboux and Gordillo. These results, therefore, show that the wedge angle given in ref 20 should be the wedge angle at the moment of droplet detachment because the angle varies continuously in time. The important conclusion from our experiments is that the wedge angle does not depend on the surface and the behavior found here is therefore universal.

Although the splashing model of Riboux and Gordillo provides a good prediction of the splashing velocity, the required calculations are rather complex: substitute eq 6 into eq 7, numerically solve for t_e, and use the result to find the splashing velocity with eq 6. Furthermore, these calculations depend on several unintuitive parameters, for instance α and λ.

Most practical situations deal with fluids with a low Ohnesorge number ($Oh \ll 1$) and take place at atmospheric conditions. Riboux and Gordillo also proposed a simplification for low Oh fluids and found an approximate splash criteria that also showed good agreement with previous experiments.[10,37] However, no detailed comparison was made between the splashing velocity prediction of both the simplification and the full-splashing model. It is unknown whether the deviation between the full splashing model and simplification is small enough to provide an accurate splashing velocity prediction with simplification. Therefore, we will follow the same approximations given by Riboux and Gordillo and compare

DOI: 10.1021/acs.langmuir.7b03355
Langmuir 2018, 34, 5163–5168

the splashing velocity given by both the full splashing model and simplification.

If we evaluate eq 2 for low Ohnesorge numbers, the first term on the left side in the equation dominates, allowing us to write the ejection time as a function of the Weber number We $\left(\mathrm{We} = Oh^2 \cdot Re^2 = \frac{\rho R v^2}{\sigma}\right)$ as

$$t_e \approx 0.88 We^{-2/3} \tag{8}$$

Consequently, the lamella thickness and spreading velocity are given by

$$V_t = \frac{\sqrt{3}}{2} v_{sp} t_e^{-1/2} = 1.07 \frac{\sqrt{3}}{2} v_{sp} We^{1/3} \tag{9a}$$

$$H_t = R \frac{\sqrt{12}}{\pi} t_e^{3/2} \approx 0.83 \frac{2\sqrt{3}}{\pi} R We^{-1} \tag{9b}$$

Further simplification can be made for the constant K_1 [eq 4]. If H_t is calculated with the measured splashing velocity and initial diameter of the drops, an average value of 7.41×10^{-6} m is obtained. Because $\lambda \approx 10^{-8}$ m, the ratio λ/H_t is in the order of 10^{-3}. As λ/H_t is small, the second logarithmic term can be approximated with the first term of the Taylor approximation

$$\ln\left(1 + 19.2\frac{\lambda}{H_t}\right) \approx 19.2\frac{\lambda}{H_t} \tag{10}$$

Because $\left|\ln\left(19.2\frac{\lambda}{H_t}\right)\right| \gg \left|19.2\frac{\lambda}{H_t}\right|$ for $\frac{\lambda}{H_t} \approx 10^{-3}$, the above term can be neglected, giving a simplified equation for K_1

$$K_1 \approx \frac{-6}{\tan^2(\alpha)} \ln\left(19.2\frac{\lambda}{H_t}\right) \approx \frac{10.69}{\tan^2(\alpha)} \tag{11}$$

The final assumption is that the lubrication force dominates over the suction force under atmospheric conditions,[20] implying that eq 5 can be simplified to

$$\beta \approx \left(\frac{K_1 \mu_g V_t}{2\sigma}\right)^{1/2} \tag{12}$$

Finally, by substituting the simplified terms of V_t [eq 9a] and K_1 [eq 11], β can be rewritten as a function of splashing velocity v_{sp}, initial diameter D_0, density ρ, surface tension σ, wedge angle α, and viscosity of the air μ_g

$$\beta \approx 2.22 \frac{\sqrt{\mu_g}}{\tan(\alpha)} (\rho R)^{1/6} \frac{v_{sp}^{5/6}}{\sigma^{2/3}} \tag{13}$$

Thus, it is possible to significantly simplify Riboux and Gordillo's splashing model for low Ohnesorge number fluids and atmospheric conditions, where the splashing ratio is only dependent on the fluid parameters and viscosity of the air, as the wedge angle seems to be identical for all smooth surfaces.

To compare the simplification with the experimental data, eq 13 can be rewritten into a simple analytical expression for the splashing velocity

$$v_{sp} = \left(\frac{\sigma^{2/3} \beta \tan(\alpha)}{2.22 \sqrt{\mu_g} (\rho R)^{1/6}}\right)^{6/5} \tag{14}$$

Then, the splashing velocity is uniquely determined by density, surface tension, and initial diameter of the droplet, viscosity of the air, wedge angle, and splashing ratio. The simplification (red dashed line), when plotted together with the experimental data and the full splashing model, as shown in Figure 3, shows good agreement. Again, the splashing ratio (β_{simpl}) was used as a fitting parameter, where the best fit value of β_{simpl} of the ethanol–water mixtures is equal to 0.120 ± 0.008, which is slightly lower than the splashing ratio of the full splashing model. This is expected as the suction force term is neglected in the simplification. For blood (red open symbols; Figure 3b), the splashing ratio also decreases ($\beta_{simpl,blood}$ = 0.112 ± 0.001), but still attains a similar value as the splashing ratio of the ethanol–water mixtures. The predicted values of the full splashing model and the simplification are similar, which shows that the simplification gives a relatively good prediction of the splashing velocity for both ethanol–water mixtures and blood.

CONCLUSION

To summarize, we systematically investigated the influence of the wetting properties of the surface on the splashing velocity of Newtonian fluid and blood (a shear thinning liquid) droplets impacting a smooth surface. We showed that the wetting properties do not influence the splashing velocity for both Newtonian fluids and blood, indicating that splashing is independent of the wetting properties of the surface. Then, we compared the experimental data with a preexisting splashing model and showed that the model can be universally applied to any smooth surface. Furthermore, the splashing model can also be used to predict the splashing velocity of blood. By measuring the wedge angle, we confirmed that the wedge angle used in the splashing model is equal to 60° at the moment of droplet detachment from the liquid sheet. Finally, we evaluated a simplification of the preexisting splashing model for low Ohnesorge number fluids at atmospheric conditions. We showed that the predictions of the simplification are comparable to the full splashing model, allowing for an easier prediction of splashing of low Ohnesorge number fluids at atmospheric conditions for any smooth surface.

AUTHOR INFORMATION

Corresponding Authors

*E-mail: T.CdeGoede@uva.nl (T.C.d.G.).
*E-mail: D.bonn@uva.nl (D.B.).

ORCID

T. C. de Goede: 0000-0003-0570-2661
D. Bonn: 0000-0001-8925-1997

Notes

The authors declare no competing financial interest.

ACKNOWLEDGMENTS

We would like to thank Detlef Lohse, who pointed us toward the work of Guillaume Riboux and José Manuel Gordillo. Furthermore, we would also like to thank José Manuel Gordillo for the useful communication regarding the splashing model.

REFERENCES

(1) Wirth, W.; Storp, S.; Jacobsen, W. Mechanisms controlling leaf retention of agricultural spray solutions. *Pestic. Sci.* **1991**, *33*, 411–420.

(2) Bergeron, V.; Bonn, D.; Martin, J. Y.; Vovelle, L. Controlling droplet deposition with polymer additives. *Nature* **2000**, *405*, 772–775.

DOI: 10.1021/acs.langmuir.7b03355
Langmuir 2018, 34, 5163–5168

(3) Shahidzadeh-Bonn, N.; Rafaï, S.; Bonn, D.; Wegdam, G. Salt crystallization during evaporation: impact of interfacial properties. *Langmuir* **2008**, *24*, 8599−8605.
(4) Lee, J. B.; Derome, D.; Carmeliet, J. Drop impact on natural porous stones. *J. Colloid Interface Sci.* **2016**, *469*, 147−156.
(5) Knock, C.; Davison, M. Predicting the position of the source of blood stains for angled impacts. *J. Forensic Sci.* **2007**, *52*, 1044−1049.
(6) Adam, C. D. Experimental and theoretical studies of the spreading of bloodstains on painted surfaces. *Forensic Sci. Int.* **2013**, *229*, 66−74.
(7) Laan, N.; de Bruin, K. G.; Slenter, D.; Wilhelm, J.; Jermy, M.; Bonn, D. Bloodstain pattern analysis: implementation of a fluid dynamic model for position determination of victims. *Sci. Rep.* **2015**, *5*, 11461.
(8) Stow, C. D.; Hadfield, M. G. An experimental investigation of fluid flow resulting from the impact of a water drop with an unyielding dry surface. *Proc. R. Soc. London, Ser. A* **1981**, *373*, 419−441.
(9) Yarin, A. L.; Weiss, D. A. Impact of drops on solid surfaces: self-similar capillary waves, and splashing as a new type of kinematic discontinuity. *J. Fluid Mech.* **1995**, *283*, 141−173.
(10) Mundo, C.; Sommerfeld, M.; Tropea, C. Droplet-wall collisions: experimental studies of the deformation and breakup process. *Int. J. Multiphase Flow* **1995**, *21*, 151−173.
(11) Bussmann, M.; Chandra, S.; Mostaghimi, J. Modeling the splash of a droplet impacting a solid surface. *Phys. Fluids* **2000**, *12*, 3121−3132.
(12) Vander Wal, R. L.; Berger, G. M.; Mozes, S. D. The splash/non-splash boundary upon a dry surface and thin fluid film. *Exp. Fluids* **2005**, *40*, 53−59.
(13) Stevens, C. S. Scaling of the splash threshold for low-viscosity fluids. *Europhys. Lett.* **2014**, *106*, 24001.
(14) Stow, C. D.; Stainer, R. D. The physical products of a splashing water drop. *J. Meteorol. Soc. Jpn.* **1977**, *55*, 518−532.
(15) Niu Wu, Z. Modélisation et calcul implicite multidomaine d'écoulements diphasiques gaz-gouttelettes. Ph.D. Thesis, Université Pierre et Marie Curie, Paris, France, 1992.
(16) Range, K.; Feuillebois, F. Influence of surface roughness on liquid drop impact. *J. Colloid Interface Sci.* **1998**, *203*, 16−30.
(17) Latka, A.; Strandburg-Peshkin, A.; Driscoll, M. M.; Stevens, C. S.; Nagel, S. R. Creation of prompt and thin-sheet splashing by varying surface roughness or increasing air pressure. *Phys. Rev. Lett.* **2012**, *109*, 054501.
(18) Xu, L.; Zhang, W. W.; Nagel, S. R. Drop splashing on a dry smooth surface. *Phys. Rev. Lett.* **2005**, *94*, 184505.
(19) Stevens, C. S.; Latka, A.; Nagel, S. R. Comparison of splashing in high-and low-viscosity liquids. *Phys. Rev. A: At., Mol., Opt. Phys.* **2014**, *89*, 063006.
(20) Riboux, G.; Gordillo, J. M. Experiments of drops impacting a smooth solid surface: A model of the critical impact speed for drop splashing. *Phys. Rev. Lett.* **2014**, *113*, 024507.
(21) Laan, N.; de Bruin, K. G.; Bartolo, D.; Josserand, C.; Bonn, D. Maximum diameter of impacting liquid droplets. *Phys. Rev. Appl.* **2014**, *2*, 044018.
(22) Lee, J. B.; Laan, N.; de Bruin, K. G.; Skantzaris, G.; Shahidzadeh, N.; Derome, D.; Carmeliet, J.; Bonn, D. Universal rescaling of drop impact on smooth and rough surfaces. *J. Fluid Mech.* **2015**, *786*, R4.
(23) Bonn, D.; Eggers, J.; Indekeu, J.; Meunier, J.; Rolley, E. Wetting and spreading. *Rev. Mod. Phys.* **2009**, *81*, 739.
(24) Karger, B.; Rand, S. P.; Brinkmann, B. Experimental bloodstains on fabric from contact and from droplets. *J. Leg. Med.* **1997**, *111*, 17−21.
(25) Merrill, E. W.; Gilliland, E. R.; Cokelet, G.; Shin, H.; Britten, A.; Wells, R. E.; et al. Rheology of blood and flow in the microcirculation. *J. Appl. Physiol.* **1963**, *18*, 255.
(26) Merrill, E. W.; Pelletier, G. A. Viscosity of human blood: transition from newtonian to non-newtonian. *J. Appl. Physiol.* **1967**, *23*, 178−182.
(27) Merrill, E. W. Rheology of blood. *Physiol. Rev.* **1969**, *49*, 863−888.
(28) *CRC Handbook of Chemistry and Physics*; Haynes, W. M., Ed.; CRC press, 2014.
(29) Vazquez, G.; Alvarez, E.; Navaza, J. M. Surface tension of alcohol + water from 20 to 50. degree. c. *J. Chem. Eng. Data* **1995**, *40*, 611−614.
(30) Bachmann, J.; Ellies, A.; Hartge, K. H. Development and application of a new sessile drop contact angle method to assess soil water repellency. *J. Hydrol.* **2000**, *231*, 66−75.
(31) Bachmann, J.; Horton, R.; Van Der Ploeg, R. R.; Woche, S. Modified sessile drop method for assessing initial soil−water contact angle of sandy soil. *Soil Sci. Soc. Am. J.* **2000**, *64*, 564−567.
(32) θ_a and θ_r are defined as the largest and smallest contact angle, respectively, a drop can attain on a surface for a constant base diameter.
(33) Young, T. An essay on the cohesion of fluids. *Philos. Trans. R. Soc. London* **1805**, *95*, 65−87.
(34) Fox, H. W.; Zisman, W. A. The spreading of liquids on low energy surfaces. i. polytetrafluoroethylene. *J. Colloid Sci.* **1950**, *5*, 514−531.
(35) Driscoll, M. M.; Nagel, S. R. Ultrafast interference imaging of air in splashing dynamics. *Phys. Rev. Lett.* **2011**, *107*, 154502.
(36) Kolinski, J. M.; Rubinstein, S. M.; Mandre, S.; Brenner, M. P.; Weitz, D. A.; Mahadevan, L. Skating on a film of air: drops impacting on a surface. *Phys. Rev. Lett.* **2012**, *108*, 074503.
(37) Palacios, J.; Hernández, J.; Gómez, P.; Zanzi, C.; López, J. Experimental study of splashing patterns and the splashing/deposition threshold in drop impacts onto dry smooth solid surfaces. *Exp. Therm. Fluid Sci.* **2013**, *44*, 571−582.

DOI: 10.1021/acs.langmuir.7b03355
Langmuir 2018, 34, 5163−5168